

Raman and SERS investigations of trihydrate amoxicillin

A. CALBOREAN*, D. MANIU, V. CHIS, T. ILIESCU, V. K. RASTOGI^a

Department of Physics, Babes – Bolyai University, M.Kogalniceanu 1, 400084 Cluj -Napoca Romania

^aPhysics Department, CCS University, Meerut-250 004, India

Raman and SERS investigations in combination with density-functional theory (DFT) were performed on the trihydrate amoxicillin (THA). The theoretical values were compared with the experimental X-ray data and Raman results. The SERS spectrum of trihydrate amoxicillin molecule on silver colloid at pH value of 6 was compared with Raman spectrum and analyzed. The adsorbed molecule is bonded to the silver surface through the amino group by chemisorption process. In adsorbed state, benzene, beta-lactam and thiazolidine rings are situated at a large distance to the silver surface and for these we presume that the electromagnetic mechanism can be implied.

(Received November 15, 2006; accepted December 21, 2006)

Keywords: SERS, SERS supports, Amoxicillin trihydrate, Density functional theory

1. Introduction

Surface Enhanced Raman Spectroscopy (SERS) is a very useful technique in surface chemistry and physics that provides greatly enhanced Raman signal from Raman-active molecules that have been adsorbed onto specially prepared metal surfaces. Increases in the intensity of Raman signal observed for molecules after adsorption on certain metal surfaces has been an interesting phenomenon both experimentally and theoretically since its discovery in 1974 by Fleischmann [1]. Usually as SERS supports, being easy to prepare, are used Ag and Au colloids. To avoid the adsorption on the metallic surface of different radicals present in colloids, solid SERS supports with nanometric structure were used as: self-assembled Ag and Au nanoparticles [2], filtration of the colloids by porous aluminium oxide with different porosity [3], colloids incapsulation in sol-gel system and polymers [4,5]

Amoxicillin is an antibiotic in the large class of penicillins [6].

Penicillin was first produced on a large scale for human use in 1943 and was used to treat infections caused by bacteria. Penicillins work by killing the bacteria or preventing their growth. But quickly, it became obvious that this drug could bear improvement because bacteria started to develop resistance to penicillin [7].

Amoxicillin is a moderate-spectrum β -lactam antibiotic used to treat bacterial infections caused by susceptible microorganisms. It is usually the drug of choice within the class because it is better absorbed, by oral administration, than other beta-lactam antibiotics. Amoxicillin is susceptible to degradation by β -lactamase-producing bacteria, and so may be given with clavulanic acid to increase its susceptibility, by inhibiting β -lactamase.

The penicillin's derivatives like amoxicillin, exert their principal antibacterial activity by binding to penicillin-binding proteins and inhibiting cell wall synthesis [8].

When the organism in a serious infection cannot be isolated, a common strategy is to attempt to cover for all possible bacteria. Amoxicillin is frequently used in combination with other antibiotics for this purpose.

For understanding the action of these drugs, it is essential to find out if the structure of the adsorbed species is similar to that of the free molecule. In this investigations, a silver surface may serve as analog for an artificial biological interface[9].

In the present paper we studied THA from experimental (Raman and SERS) and theoretical (DFT) point of view. Semiempirical and (DFT) calculations were compared with the experimental X-ray data and Raman results.

The Raman spectra obtained from trihydrate amoxicillin in powder form, solution and adsorbed on the colloidal silver particle have been recorded and analyzed.

These investigations may be considered starting points for further medical studies in order to identify optimal strategies for specific infections.

2. Experimental

2.1. Sample and instrumentation

The amoxicillin and all other materials involved in substrate and sample preparation were purchased from commercial source as analytical pure reagents. A yellow silver sol solution has been obtained according to literature[10]. In brief, 15 ml of 10^{-3} mol⁻¹ AgNO₃ to 50 ml of 2×10^{-3} mol⁻¹ Na[BH₄] solution kept at ice-water temperature. The mixture was then strongly stirred for half an hour. The obtained colloid was yellowish with an absorption maximum at 423 nm. Small amounts of trihydrate amoxicillin 10^{-3} M water and methilic alcohol solution were added to 2 ml silver colloid using a micropipette. KCl solution (1,5 M) was also added (10:1)

to obtain the sol coagulation [11]. The Raman and SERS spectra were recorded on a GDM 1000 double monochromator. The excitation line 514 nm (200Mw) from an argon ion laser Innova 90. The FT-Raman spectrum of the solid state trihydrate amoxicillin was recorded using a Bruker Equinox 55 spectrometer with an integrated FRA 106 Raman module and a resolution of 2 cm^{-1} . Radiation of 1064 nm from Nd-YAG laser was employed for excitation. UV visible absorbtion spectra of THA and silver colloid were recorded with a Perkin Elmer Lambda 19 UV- VIS-NIR spectrometer with a scan speed of 240nm/min.

2.2. Computational details

The molecular geometry optimisations and vibrational frequencies of the investigated compound were performed using the Gaussian 98 software package by the B3LYP DFT [12] method in conjunction with the split valence shell 6-31G(d) basis set [13]. To compare the calculated vibrational frequencies with the experimental counter – parts the former was scaled with the recommended frequency scalling factor 0.96414 [14]. The convergence of all the calculations and the absence of imaginary values in the wavenumbers prove that a local minimum on the potential energy surface was found.

3. Results and discussion

3.1. Theoretical calculations

The schematic structure of trihydrate amoxicillin with the labeling of the atoms is illustrated in Fig1. The DFT calculations have been accomplished on THA using the B3LYP method in conjunction with the split valence shell 6 -31G (d) basis set.. The selected calculated strucutral paramaters are given in Table1 together with the available X-ray data. As one can remark from Table 1, the calculated bond lengths and bond angles are in agreement with the experimental X-ray data, the observed difference between dihedral angles being most probably due to the intermolecular interactions, wich occur in the crystal.

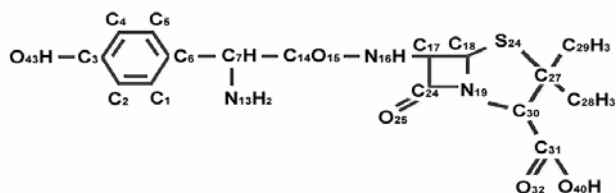


Fig. 1. Schematic structure of the trihydrate amoxicillin salt with the labeling of the atoms.

In addition, the theoretical calculations were performed for the gas phase, while the experimental data were for solid phase.

Table 1. Selected calculated bond lengths (Å) and angles (degree) of trihydrate amoxicillin compared with the experimental data.

Bond length (Å)	Calc.	Exp.
C1 - C2	1.392	1.385
C2 - C3	1.401	1.371
C3 - C4	1.396	1.375
C4 - C5	1.393	1.369
C5 - C6	1.401	1.371
C6 - C7	1.530	1.511
C7 - N13	1.462	1.472
C7 - C14	1.538	1.517
C14 - O15	1.225	1.222
C14 - N16	1.370	1.344
N16 - C17	1.427	1.425
C17 - C18	1.568	1.519
C18 - N19	1.471	1.368
N19 - C24	1.402	1.495
C24 - C17	1.552	1.562
C24 - O25	1.204	1.192
N19 - C30	1.452	1.458
C30 - C27	1.586	1.556
C27 - S26	1.879	1.845
S26 - C18	1.839	1.779
C27 - C28	1.533	1.504
C27 - C29	1.539	1.513
C30 - C31	1.527	1.547
C31 - O32	1.206	1.221
C31 - O40	1.358	1.257

Angles (degree)	Calc.	Exp.
C1 - C2 - C3	120	119.1
C2 - C3 - C4	119.8	121.6
C3 - C4 - C5	119.6	118.7
C4 - C5 - C6	121.5	120.2
C5 - C6 - C7	120.8	121.5
C6 - C7 - N13	115.8	111.3
C7 - N13 - C14	37.4	35.9
C7 - C14 - O15	121.9	121.4
C14 - O15 - N16	30.3	124.6
C14 - N16 - C17	122	123
N16 - C17 - C18	120.8	114.6
C17 - C18 - C24	47.7	84.7
O25 - C24 - N19	131.3	130.7
C18 - N19 - C24	93.1	46
N19 - C18 - C30	30.8	117.4
C18 - S26 - N19	32.9	103.4
S26 - C27 - C30	104.3	104.9
C30 - C31 - O32	126.3	114.8
O32 - C31 - O40	123.4	126
C31 - C30 - C27	111.9	114.2
C27 - C29 - C28	34.6	35.15
C27 - C29 - S26	39.5	31.5
O25 - C24 - C17	136.8	135.5
C3 - O43 - C4	31.6	116.6

Dihedral angles	Calc.	Exp.
N13 - C7 - C14 - O15	33.3	-150.5
N16 - C14 - O15 - C7	-177.5	172.6
C2 - C3 - O43 - C4	179.9	-178.9
O15 - C14 - N16 - C17	1.3	1
C14 - N16 - C17 - C24	-143.8	-129.2
C6 - C1 - C5 - C4	-179.9	-0.4
N19 - C30 - C18 - S26	153.4	-26.2
O25 - C24 - N19 - C30	-34.7	-37.3
C18 - C17 - N16 - S26	-14	162.5
S26 - C18 - N19 - C24	103.6	109.2
C17 - N16 - C18 - C24	-46	115
O32 - C31 - C30 - C27	-100.4	118
O15 - C14 - N16 - C7	177.7	-172.6

The Fig. 2 present the solid state Raman spectrum of THA compared with theoretical spectrum.

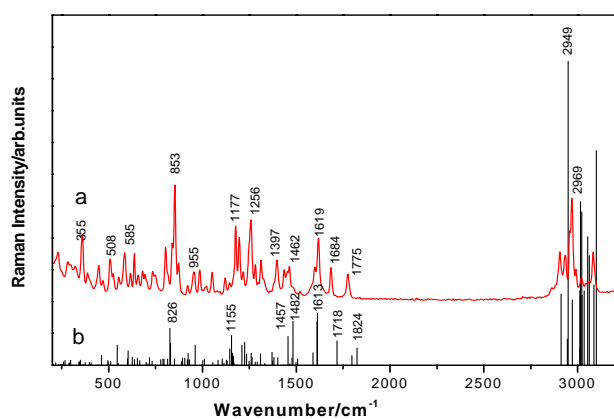


Fig. 2. Raman spectra of the trihydrate amoxicillin salt: Solid spectrum (a) and theoretical spectrum (b).

The obtained Raman bands together with theoretical frequencies and their assignments are presented in Table 2. As can be seen from Table 2, the theoretical calculations match well with the experimental data and allow the assignment of the vibrational modes.

The most intense bands appears at the 2969 (2949) and 853 (851) cm^{-1} (theoretical values are given in parenthesis) and are determined by the symmetric stretching vibrations of C28H3 and C29H3 bonds and by beta lactam and thiazolidine rings in plane deformation (see Fig. 1, for structure with the labeling of the atoms). Other intense bands, which are due to the bending of C3H and C30H in addition with OH bending of COOH can be observed at 1196 (1185) and 1256 (1260) cm^{-1} . The phenyl ring breathing vibration determines weak bands at 616 (626) and 986 (995) cm^{-1} . In plane deformation of phenyl ring in addition to the deformation of the amino group are presented at 1619 (1613) cm^{-1} . The thiazolidine ring, in- plane deformation can be observed with a medium intensity in the spectral range between 448 (443) and 508 (511) cm^{-1} in addition to a bending of the secondary amide group given by N16H group.

The OH vibration of the COOH group gives the medium-weak bands at 616 (603) cm^{-1} and 656 (653) cm^{-1} . Another intense band at 1177 (1181) cm^{-1} is determined by bending vibrations of (C7H), (C18H), (N16H), in addition with twisting vibration of N13H2 amino group.

Table 2. Raman (experimental and calculated) and SERS wavenumber (in cm^{-1}) of trihydrate amoxicillin with their vibrational assignments.

Raman Solid sample (cm^{-1})	Raman Solution (cm^{-1})	Calc. (cm^{-1})	SERS NaBH ₄ (cm^{-1})	Vibrational assignment
228 w	237 shw	234	252 s	$\delta(\text{CH}_3)+\delta(\text{C}24\text{O}25)+\text{ring1}$ in plane def.
282 w	-	288	284 m	$\delta(\text{CH}_3) + \delta(\text{N}16\text{H}) + \text{r}(\text{N}13\text{H}2) + \delta(\text{C}7\text{H}) + \text{ring2}$ in plane def.
298 sh	-	298	308 w	$\delta_{\text{as}}(\text{CH}_3)$
359 s	-	364	374 w	$\delta(\text{CH}_3)+\delta(\text{C}30\text{H}39)$ +COOH def.
386 w	391 m	376	-	CH ,OH ring1 out of plane.+ r(N13H2)+ (N16H)+COOH def.
398 w	-	398	-	$\delta(\text{N}16\text{H})\text{def} + \text{CH ring1}$ in plane def+OH def. of COOH + t(N13H2) + ring2 in plane def.
-	30 shm	-	415 w	-
448 m	-	443	-	(N16H)def.+ $\delta_{\text{as}}(\text{CH}_3)+\text{ring}2,3$ in plane def.
469 w	-	462	-	$\delta(\text{N}16\text{H})$ def
-	485shm	497	-	$\delta(\text{N}16\text{H})\text{def.}+\text{OH def. of COOH} +\text{ring3}$ in plane def.
508 m	-	512	519 m	ring1 out of plane + $\delta(\text{N}16\text{H})\text{def}+\text{ring}2,3$ in plane def. + $\delta(\text{CH}_3)+\text{COOH def.}$
523 shw	-	-	-	-
554 w	-	551	-	CH ring1 in plane def +w(N13H2)+ OH def.of COOH
585 m	-	600	-	ring 2 out of plane + OH def. of COOH
-	603 shw	604	-	OH def. of COOH + $\delta_{\text{as}}(\text{CH}_3)+\text{ring3}$ in plane def.
616 w	-	626	616 w	ring 1 breathing
637 m	-	638	-	OH def. of COOH+ $\delta(\text{C}17\text{H})+ \delta(\text{C}18\text{H})+ \delta(\text{CH}_3)$
656 w	-	653	-	OH def of COOH+ $\delta(\text{C}18\text{H})+\text{ring}2,3$ in plane def.
681 w	-	-	673 w	-
693 w	697 w	700	-	ring1 out of plane+ t(N13H2)+ $\delta(\text{C}17\text{H})+ \delta(\text{C}18\text{H})$
735 w	-	732	-	ring1 in plane def+ $\delta(\text{N}13\text{H}2)+\delta(\text{C}7\text{H})+ \delta(\text{C}17\text{H})+ \text{OH def. of COOH}$
749 w	-	-	754 w	-
-	788w	790	793 w	CH ring 1 in plane def.
803 m	-	795	-	CH ring 1 in plane def +

Raman Solid sample (cm ⁻¹)	Raman Solution (cm ⁻¹)	Calc. (cm ⁻¹)	SERS NaBH ₄ (cm ⁻¹)	Vibrational assignment
				w(N13H2)+ δ (N16C14C7)
838 sh	-	830	824 w	CH ring 1 in plane def. + δ (N13H2) + δ (C30H) + ring2 in plane def.
853 vs	-	851	-	ring2,3 in plane def. +v(C24C17C18N19)+ δ (C30H) + OH def of COOH
872 w	879 w	889	863 w	w(N13H2) + δ (C7H)+ CH ring 1 in plane def.
921 w	-	920	-	CH ring 1 in plane def
953 w	-	962	939 m	δ (C17H) + δ (C18H) ring2 in plane def
986 w	-	1000	-	ring 1 breathing
1021 w	1018 vs	1011	1012 w	δ (CH3) osc+v(C24C17)+ δ (C30H)+ring2 in plane def
1052 w	-	1055	1043 m	δ (C30H) + δ (C17H) + δ (C18H) + δ (C24N19) +w(N13H2)
1081 shw	1078 m	1084	1088 w	CH ring 1 in plane def+w(N13H2)+ δ (C7H)
1121 w	1118 w	1128	-	δ as(CH3)+ δ (C18H)
1145 w	-	1146	1162 s	δ (C17,H) + δ (C18,H)
1177 s	-	1181	-	δ (C7H) + δ (C18H) + δ (N16H) + t(N13H2)
1196 s	-	1185	-	δ (C3H) osc + OH def.of COOH
1216 w	-	1211	-	δ (C17,H) + δ (C18H) + ring2 in plane def.+ t(N13H2)
-	1234 w	1225	1233 m	t(N13H2) + δ (N16H) + δ (C7H)
1258 s	-	1260	-	δ (C30,H) + δ (OH) of COOH + δ (CH3)osc.
1281 w	1280sh	1281	1291 m	ring2 in plane def.+ δ (C17H)+ δ (C18H) + δ (OH) of COOH
1312 m	-	1310	-	δ (C17,H) + δ (C18H) + δ (N16H) + t(N13,H2) + ring2 in plane def.
1324 sh	-	1332	-	δ (OH) + δ (CH) ring1 in plane def.+ δ (C7,H)
-	-	1370	1353 vs	t(N13,H2) + δ (C7,H)
1397 m	-	1402	-	δ s(CH3)
1435 m	-	1436	1446 s	δ (OH) + δ (CH) ring1 in plane def+ δ (C7,H)
1453 sh	1452 s	1457	-	δ as(CH3)
1462 m	-	1465	-	δ as(CH3)
1480 sh	-	1482	-	δ as(CH3)
1518 w	-	1507	-	CHring1 in plane def+(CC) ring1 in plane def+ δ (N16H)
-	-	-	1555 w	-
-	1581 m	1589	-	(CH,OH) ring 1 in plane def.
1599 m	-	-	1606 s	-
1619 s	-	1613	-	δ (CH,OH) ring 1 in plane def. + w(N13H2)
-	-	-	1643 w	-

Raman Solid sample (cm ⁻¹)	Raman Solution (cm ⁻¹)	Calc. (cm ⁻¹)	SERS NaBH ₄ (cm ⁻¹)	Vibrational assignment
1684 m	-	1719	-	δ (N13H2) + v(C14O15) + δ (C7,H) + δ (N16H)
-	-	-	1746w	-
1775	-	1797	-	v(CO) of COOH
2969	-	2945	-	vs (C29H3) + vas (C28H3)

v, very; w, weak; m, medium; s, strong; sh, shoulder; δ , scissoring; w, wagging; t, twisting; v, stretching; ring 1, phenyl ring; ring 2, beta-lactam ring; ring 3, thiazolidine ring; Calc, calculated with B3LYP / 6-31 g (D)

4. Adsorption on silver surface

The SER spectrum of THA compared with solid state Raman spectrum is represented in Fig. 3. Another intense band at 1177 (1181) cm⁻¹ is determined by bending vibrations of (C7H), (C18H), (N16H), in addition with twisting vibration of N13H2 amino group.

The pH value of 6 was selected for colloid solution to be the same as in the human body. Also, it is known that in acidic and basic environments, THA molecule can be broken [15]. SERS and Raman bands together with their assignment are summarized in Table 2.

It has been generally accepted that the contribution to the overall enhanced Raman signal is given by two different mechanisms.

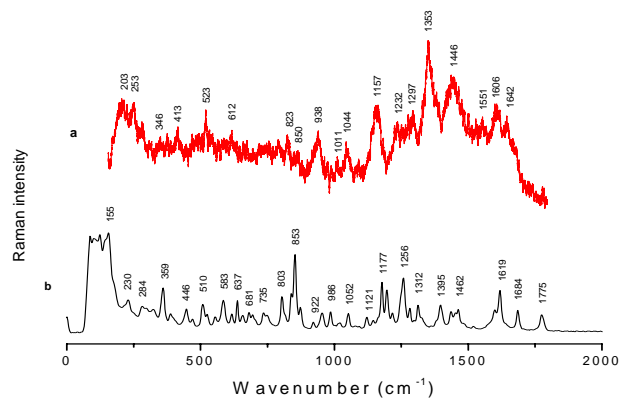


Fig. 3. Raman solid state spectrum (a) of trihydrate amoxicillin and SERS spectrum (b) at pH6. Excitation line 514 nm, laser power 200mW.

The electromagnetic enhancement is dependent on the presence of the metal surface's roughness features and is caused by resonance excitation of the surface plasmon [16].

The chemical mechanism is based on the formation of a charge – transfer complex between the surface and analyte [17].

A major contribution to the observed enhancement is given by the electromagnetic mechanism however chemical enhancement also plays a significant role, these two mechanisms being difficult to separate [18].

As observed in Fig. 3 there are several changes in the relative intensities of some bands in the SER spectrum as compared to the normal Raman spectrum. Hereby, the bands at 1350, 1446, and 1157 cm^{-1} become the most intense in the SER spectrum, while the intensity of the band located at 863 cm^{-1} is very weak in comparison to the bulk Raman spectrum. The SER spectrum includes a large background between 1200 and 1600 cm^{-1} . This background [19] is probably due the photo or thermal decomposition of THA which forms carbon layers on silver. Moreover, shifts of some SERS bands compared to the corresponding Raman bands can also be observed, which demonstrate the chemisorption process of the THA molecule through some of its constituent groups, while other groups are situated at a relatively large distance from the metal surface, their vibrations being slightly influenced by adsorption. For example, the weak intensity of the bands specific to the phenyl ring at 626 cm^{-1} , or beta-lactam and thiazolidine rings at 519 cm^{-1} in the SER spectrum prove that these rings are situated at a large distance from metal surface. The twisting vibration of amino group at 1350 cm^{-1} being very strong allow us to suppose that the THA molecule is bonded to silver surface by this group.

A evaluation of adsorbate orientation and hence the surface binding geometry of THA can be obtained from by using surface selection rules[20]. In agreement with these rules, if the z-axis is normal to the surface, then vibrations of the adsorbed molecule, which have a polarizability tensor component along this axis, will be preferential enhanced.

The bonding of THA to the silver surface can be accomplished through different atoms. The absence in the SER spectrum of the bands due to vibrations in which the sulfur atom from thiazolidine ring is implied (Table 2) allows us to assume that this atom is not involved in the THA adsorption on the silver surface.

The very strong intensity of amino N_{13}H_2 band (1350 cm^{-1}) in the SER spectrum owing to twisting vibration (the movement of atoms are perpendicular to respect to the surface indicate that this group lies in the proximity of the silver surface. On the other hand, the very weak intensity of the bands N_{16}H band in the 448-508 cm^{-1} spectral region determined by the vibration of this group is a proof that this group is not implied in the adsorption on the silver surface.

The presence of carbonyl group ($\text{C}_{14}\text{O}_{15}$) in vicinity of the amino N_{13}H_2 group (Fig. 1), is an indication of the possible involvement of this group in the molecule adsorption.

Because of very weak intensity of the carbonyl group bands, we presume that the adsorption of THA molecule is most probably due by NH_2 amino group.

The very weak intensities of the SERS bands attributed to the deformation of phenyl ring, (Table 2) in the 749-838 cm^{-1} spectral range is a consequence of the relatively large distance of this ring relative to the metal surface.

The absence in the SER spectrum of the bands (386 cm^{-1} , 398 cm^{-1}) due to vibrations in which the COOH

group is involved demonstrate also that this group is at a large distance from the silver surface surface.

By taking into account all these considerations, it becomes obvious that the THA species are adsorbed on the silver surface through the amino group.

In the fig.4 is presented the optimized geometry of the THA molecule with the most probable adsorption.

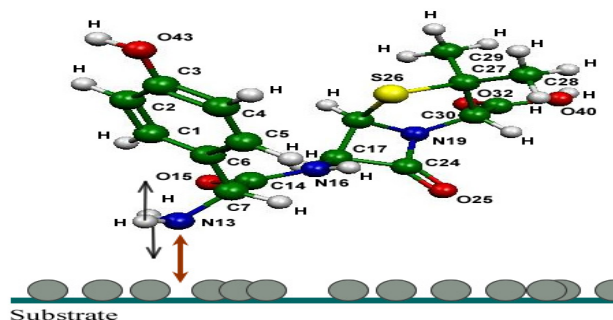


Fig. 4. Optimized geometry of the trihydrate amoxicillin molecule with the adsorption on the silver surface by the amino group.

In order to understand the adsorption behavior of the THA species on the metal surface, and to get insights about the SERS enhancement mechanism, electronic absorption spectra (Fig. 5) of pure THA solution, silver colloid and mixture of activate silver sol in addition with THA were recorded.

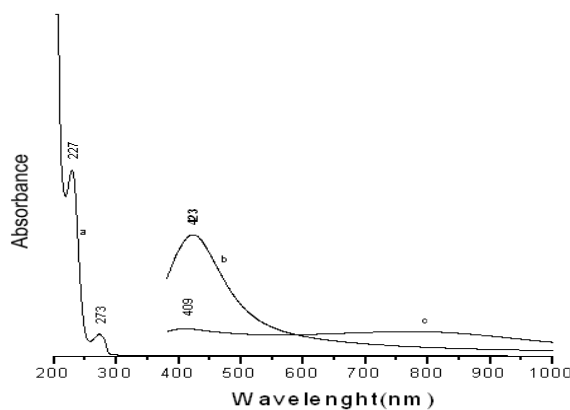


Fig. 5. Absorption spectra of trihydrate amoxicillin salt: 2.5×10^{-3} water and methanol solution (a), pure silver colloid (b), 2.5×10^{-3} trihydrate amoxicillin solution and 10^{-1} M KCl (c).

As one can see, the free THA species have an absorption maximum in UV spectral range (fig.5a) induce no resonant contribution is expected to the enhancement of the SERS bands.

The spectrum of pure silver colloid (Fig5.b) shows a single absorption maximum at 423 nm and is given by small particle plasma resonance.

The addition of THA and KCl to the silver sol (Fig5c) determines a significant diminution of this absorption band and the appearance of a new broad absorption band around 800 nm.

The second absorption peak arise from the aggregation of the colloid particles

The major changes evidenced between the Raman and SER spectra of THA molecule corroborated with the features of the absorption spectrum of activated solver sol with allow us to presume the chemisorption of the THA species on the colloidal silver particles and the contribution of the charge – transfer effect to the overall SERS enhancement.

5. Conclusions

Raman and SERS investigations have been accomplished in combination with DFT theoretical calculations on the trihydrate amoxicillin. The theoretical calculated values of the molecule structural parameters reproduce well the experimental X-ray diffraction data. The assignment of vibrational modes was performed on the basis of the theoretical calculations and a fairly good agreement between experimental and theoretical data was achieved. The chemisorption process was observed, trihydrate amoxicillin molecule being bonded on the silver surface by amino group. The phenyl, beta-lactam and thiazolidine rings are situated at large distance with respect to the silver surface.

References

- [1] M. Fleischmann, P. J. Hendra, A. M. McQuillan, *Chem.Phys.Lett.* **26**, 163 (1974).
- [2] Wei Wang, B. Gu, *Applied Spec.* **59**,1509, (2005).
- [3] W. S. Sutherland, J. D. Winefordner, *J. of Colloid and Interface science* **148**, 129 (1992).
- [4] A. Brioude, F. Lequevre, J. Mugnir, J. Dumas, G. Guiraud, J. C. Plenet, *J. of Applied Spec.* **88**, 6187 (2000).
- [5] S. Porel, S. Singh, S. Harsha, D. Rao, T. P. Radhakrishnan, *Chem. Mater.* **17**, (2005).
- [6] T. Iliescu, M. Baia, I. Pavel, *J. Raman Spectroscopy* **37**, 318, (2006)
- [7] H. C. Neu, M. D. P &S Medical Review, Vol. 1, No.1 (1993).
- [8] Christopher Walsh, *Nature* Vol. 406, 775, 2000.
- [9] C. G. Dryhurst, *Electrochemistry of Biological Molecules*, Academic Press, New York, (1977).
- [10] T. Iliescu, M. Vlassa, M. Caragiu, I. Marian, S. Astilean, *Vib. Spectroscopy*, **8**, 451, (1995).
- [11] K. Kneipp, H Kneipp, G.Deinum, I.Itzkan, *Applied Spectroscopy* Vol. 52, No.2, 175,(1998).
- [12] A. D. Becke, *Phys.Rev* **A38**:3098, (1988).
- [13] M. J. Frisch, G. W. Trucks, Schlegel, Scuseria, Cheeseman J. R., Zakrzewski, J. A. Montgomery Jr, R. E. Stratmann, J. C. Burant, S. Dappprich, J. M. Millam, A. D. Daniels, K. N. Kudin, M. C. Strain, O. Farkas, J. Tomasi, V. Barone, M. Cossi, R. Cammi, B. Mennucci, C. Pomelli, C. Adamo, S. Clifford, J. Ochterski, G. A. Petersson, P. Y. Ayala, Q. Cui, K. Morokuma, D. K. Malick, A. D. Rabuck, *Gaussian 98, Revision A7, Gaussian: Pittsburgh, PA* (1998).
- [14] J. Antony, S. Burkhard, C. Schutte, *J. Chem. Phys.* **122**, 014309, (2005)
- [15] A. Liese, K. Seelbach, C. Wandrey, *Industrial biotransformation*, Wiley VCH, Verlag GmbH, Weinheim (2001)
- [16] Z. Zhu, T. Zhu, Z. Liu, *Nanotechnology* **15**, 357, (2004)
- [17] M. C. Chen, S. Tsai, M. Chen, S. Y. Qu, W-H. Li, K. L. Lee, *Phys. Rev. B* vol 51, 4507, 1995
- [18] M. Moskovits, Lella DP. *J. Chem. Phys.* **73**, 6088 (1980)
- [19] S. T. Oh , K. Kim, M. S. Kim, *J. Phys. Chem.* **95** 8844 (1991)
- [20] Osawa, Masatoshi, Ataka, Ken-Ichi, Yoshii, Katsumasa, Nishikawa, Yuji, *Appllied Spec.*, **47**(9), 1497 (1993).

*Corresponding author: ilitra@phys.ubbcluj.ro